ORIGINAL ARTICLE

Solvent free oxidation of ethylbenzene over Ce-BTC MOF

CrossMark

Mei Mei Peng, Mani Ganesh, Rajangam Vinodh, Muthiahpillai Palanichamy, Hyun Tae Jang *

Department of Chemical Engineering, Hanseo University, 360 Daegok-ri, Haemi-myun, Seosan 356-706, Chungcheongnam-do, South Korea

Abstract   A cerium based metal–organic framework (MOF) Ce-BTC (BTC = 1,3,5-benzenetricarboxylic acid) was synthesized using a solvothermal route and was characterized via powder XRD, BET, SEM, TGA, DRS-UV–vis, FT-IR, and ESR analyses. Oxidative catalytic performance of the synthesized catalyst was evaluated using ethylbenzene oxidation under optimum conditions. The results obtained suggest that the catalyst was efficient in the oxidation of EB with 84.99% conversion and 95.63% selectivity.

© 2014 The Authors. Production and hosting by Elsevier B.V. on behalf of King Saud University. This is an open access article under the CC BY-NC-ND license (http://creativecommons.org/licenses/by-nc-nd/3.0/).

1. Introduction

Abundant, industrially valuable synthetic organics are commonly derived through oxidation from cheap hydrocarbons. With respect to this, a wide variety of heterogeneous catalysts have been studied in the aerobic oxidation of hydrocarbons. Oxidative derivatives of ethylbenzene (EB) have found applications in the synthesis of economically valuable chemicals and monomer materials (Habibi et al., 2013). Heterogeneous catalysts, such as mesoporous silica (Shrikant et al., 2006), zeolite (Bennur et al., 2004), and metal-containing heterogeneous

solid acid catalysts (Keigo et al., 2004; Vasant et al., 2004) have been studied for their ability to oxidize alkyl aromatics due to their inherent advantages, such as ease of recovery, recyclability of the catalyst, and suitability for a continuous process. Ceria-aided oxidation of alkyl aromatics has been studied extensively by various researchers (Zhao et al., 2006; Araujo et al., 2003).

Acetophenone is an oxidative product of EB that has found applications as an intermediate in the synthesis of many value-added products (Kroschwitz et al., 1995; Nicholson and Adams, 1968; Baver and Garbe, 1985). Liquid phase oxidation of EB using transition metal catalysts, such as Co, Mn, Fe, and Cu, were studied. 8-Quinolinolato manganese (III) complexes were also reported to catalyze EB oxidation, but the use of that material resulted in poor conversion (Lu et al., 2010). Recently, a heteropolytungstate catalyst in the presence of H_2O_2 was found to achieve 93% EB conversion (Kanjina and Trakarnpruk, 2010), but the method suffers from high cost of the catalyst and using unstable H_2O_2 as the oxidant. A

Ce-incorporated AlPO-5 catalyst was studied recently, and it was reported to be more effective for the vapor-phase oxidation of ethylbenzene (Subbiah et al., 2011). However, vapor phase oxidation may suffer from backpressure during the reaction, and coke formation inside the catalyst can reduce catalyst recyclability.

Over the past decade, numerous metal–organic framework (MOF) materials have been devised for gas adsorption and storage (Ma and Zhou, 2010), sensing (Hadi et al., 2013), drug delivery (Jihyun et al., 2009), and separation (Emmanuel et al., 2010). MOF structures are constructed by the combination of metal ions or clusters with polytopic organic ligands, which lead to structural characteristics such as high surface area, porosity, chemical tenability, flexibility, and structural diversity. These attractive properties have made MOFs increasingly interesting in the field of catalysis (David et al., 2009). Various organic reactions, such as alkene epoxidation (Song et al., 2010), cyanosilylation (Mikaela et al., 2010), hydrogenation (Isaeva et al., 2013), Suzuki cross-coupling (Françesc et al., 2007), aza-Michael condensation (Lien et al., 2012), the Sonogashira reaction (Gao et al., 2010), transesterification reactions (Zhou et al., 2009), Friedel–Crafts alkylation and acylation (Lien et al., 2011), and oxidation (Zhang et al., 2013) were studied using MOFs as catalysts. Recently, some studies have been devoted to study the performance of MOFs as catalysts in the oxidation of EB (Lida and Faezeh, 2013; Luz et al., 2013), but not extensively. Matthias et al., (2014) have studied the oxidation extensively using a vanadium based MOF (MIL-47) for oxidation of cyclohexene through epoxidation reaction. They studied the effect of the group substituted (OH, F, Cl and Br) on BDC (benzene dicarboxylic acid linker). They found that the alkylperoxo species formed on the vanadia site is more reactive and responsible for oxidation (Matthias et al., 2014). As discussed above, ceria is an excellent material for the oxidation of alkyl aromatics, but until now ceria-based MOFs have not been studied for EB oxidation. Ce-based MOF was first reported by Almáši et al., synthesized using BTC as linker. In Ce-BTC the oxygen atom of each carboxylate group of the BTC ligand is coordinated to Ce(III) cations. Further the central Ce atom is linked with one molecule of water by coordination which will fulfill the coordination Ce atom. Further the bond length Ce-O of seven coordinated oxygen atoms was found in the range of 2.38–2.53 Å. One more oxygen atom linked with the CeO_8 sphere was found as semicoordinated. Hence altogether they formed a coordination polyhedron around Ce with bi-capped trigonal prism. The shape of the MOF and presence of Ce atom in its Ce^{3+} state will give hope to evaluate its oxidation capabilities. To our knowledge, there is no reported study on the oxidation of EB using a Ce-BTC framework. Thus, in our present report, we studied the catalytic performance of Ce-BTC in liquid phase oxidation of EB in solvent–free conditions.

2. Experimental

2.1. Synthesis of the catalyst

Ce-BTC was synthesized via a solvothermal reaction in a typical synthesis run. Thus, 6 mmol (1.26 g) BTC and 10 mmol (4.34 g) cerium nitrate hydrate were dissolved in 60 mL DMF. Then, the mixture was sealed in a 100 mL Teflon-lined stainless steel autoclave and heated at 130 °C for 24 h. After cooling to room temperature naturally, the product was filtered, washed with DMF, and vacuum-dried at 50 °C (Scheme S1).

2.2. Characterization of the catalyst

Powder XRD patterns were recorded using a Rigaku D/Max 2200 + Ultima diffractometer with Cu-Kα radiation (λ = 0.154 nm). Diffraction data were recorded in the 2θ range 5–30° at a step of 0.02°/s. TGA was performed using a Scinco TGA N-1000 thermo gravimetric (TG) analyzer. The S_{BET} and pore volume were measured with a BEL-Belsorp II volumetric adsorption analyzer. Prior to each adsorption measurement, the samples were evacuated under vacuum ($p < 10^{-5}$ mbar) at 105 °C for 6 h. SEM images were captured on a JEOL JSM 5600 scanning electron microscope. Ultraviolet–visible diffuse reflectance (DRS UV–vis) spectra were recorded on a SCINCO Neosys 2000 spectrometer. Fourier transform infrared (FT-IR) spectra were recorded at room temperature with 4 cm^{-1} resolution between 4000 and 400 cm^{-1} with an FT-IR spectrometer (Nicolet IR 200). The electron spin resonance (ESR) spectrum was recorded on a JES-TE200 (JEOL, Japan) instrument with a microwave frequency of 9.4 Hz.

2.3. Catalytic reaction

The catalytic activity and selectivity of the oxidation of ethylbenzene (EB) were studied in solvent-free conditions. For this, we followed a method reported in prior studies (Raju et al., 2008) with some modifications. In a typical run, 5 mL EB and 0.10 g catalysts were taken in a 50 mL round
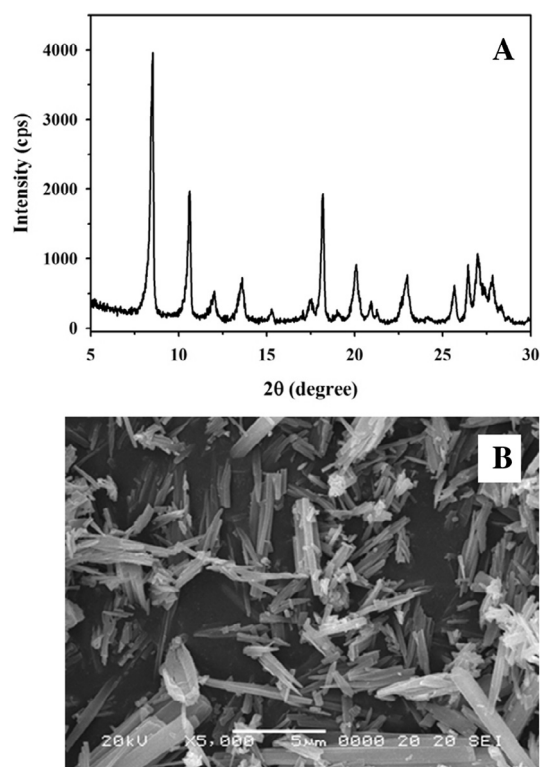

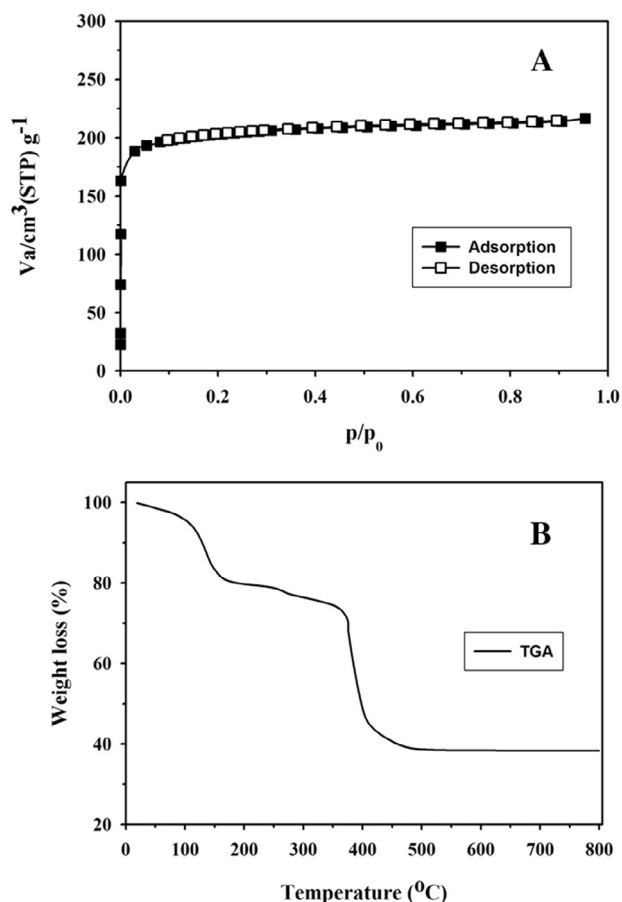**Figure 1** (A) XRD pattern of Ce-BTC, (B) SEM image of Ce-BTC.

Figure 2 (A) Nitrogen adsorption–desorption isotherms of Ce-BTC, (B) TGA curve of Ce-BTC.

bottom flask with a water-cooled reflux condenser and an O_2 gas inlet. The mixture was heated at a constant temperature and with continuous O_2 gas flow of 5.5 mL/min with stirring for 6 h. The evaporated EB becomes condensed with the aid of an attached water-cooled reflex condenser, so only excess O_2 after the reaction will escape through the needle attached over the condensed plug (the reaction set-up is shown in Supplementary file Fig. S1). Then, the reaction mixture was cooled to room temperature and filtered to remove the catalyst. The recovered catalyst was recycled by washing it with ethanol and then drying it. The reaction products were analyzed via GC (Agilent, HP-5 column, 50 m × 320 μm × 0.52 μm and FID detector).

3. Results and discussion

3.1. Characterization of catalyst

The results of the powder XRD are shown in Fig. 1(A). The peaks that appeared at 8.4, 10.6, and 18.1 (2θ) revealed that the crystallinity of the Ce-BTC obtained was good and comparable to that reported in prior literature (Nazmul et al., 2010). The peaks in XRD of Ce-BTC synthesized here are similar to that of the Ce-BTC in the earlier reports (Almáši et al., 2010). The SEM image (Fig. 1(B)) showed that the Ce-BTC catalyst displayed needle-shaped particles, 10–20 μm in size, and with smaller broken particles (Nazmul et al., 2010; Luo et al., 2008).
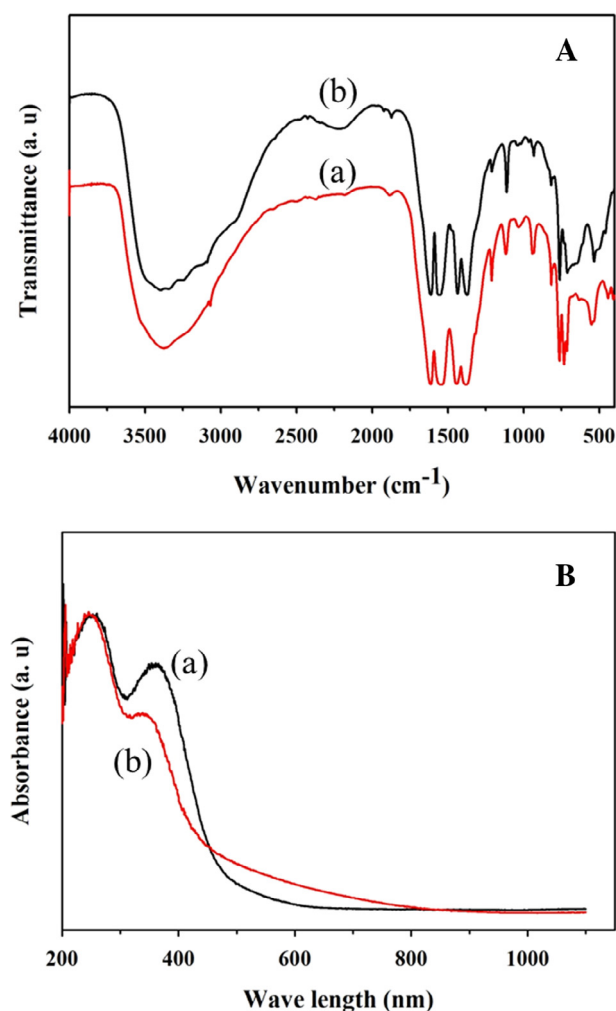

Figure 3 (A) FT-IR spectra of (a) Ce-BTC, (b) Ce-BTC after reaction, (B) DRS-UV spectra of (a) Ce-BTC, (b) Ce-BTC after reaction.

Fig. 2(A) shows the N_2 adsorption–desorption isotherms of Ce-BTC, with a type I isotherm for micropore materials with 778.5 $m^2 g^{-1}$ of surface area and 0.3346 $m^3 g^{-1}$ of pore volume. Fig. 2(B) shows the TGA result of Ce-BTC. There was a minor weight loss at 100 °C, due to loss of physically adsorbed and lattice coordinated water, further a slow weight loss was observed until 300 °C which may be due to the solvent DMF and water coordinated with the pores of MOF and the next major weight loss occurred at around 350 °C, due to the decomposition of the Ce-BTC framework. Thus, the catalyst is stable up to about 350 °C, which is similar with that of Almáši et al. report (2010) on Ce-MOF. (Almáši, M., Zeleňák, V., Císařová, I., A. Bell. A novel cerium metal-organic framework. http://photon-science.desy.de/annual_report/files/2010/20101138.pdf. (accessed on 15/12/2013)).

The FT-IR spectrum of the synthesized Ce-BTC is shown in Fig. 3(A). The intense band observed at around 3450 cm^{-1} was assigned to the OH stretching of water molecules, which may be physically adsorbed or bonded (coordinated). Water peaks can also be observed even when the product was dried at 150 °C for 1 h, which is due to KBr pellet preparation in an atmosphere of air, so the MOF may capture water molecules
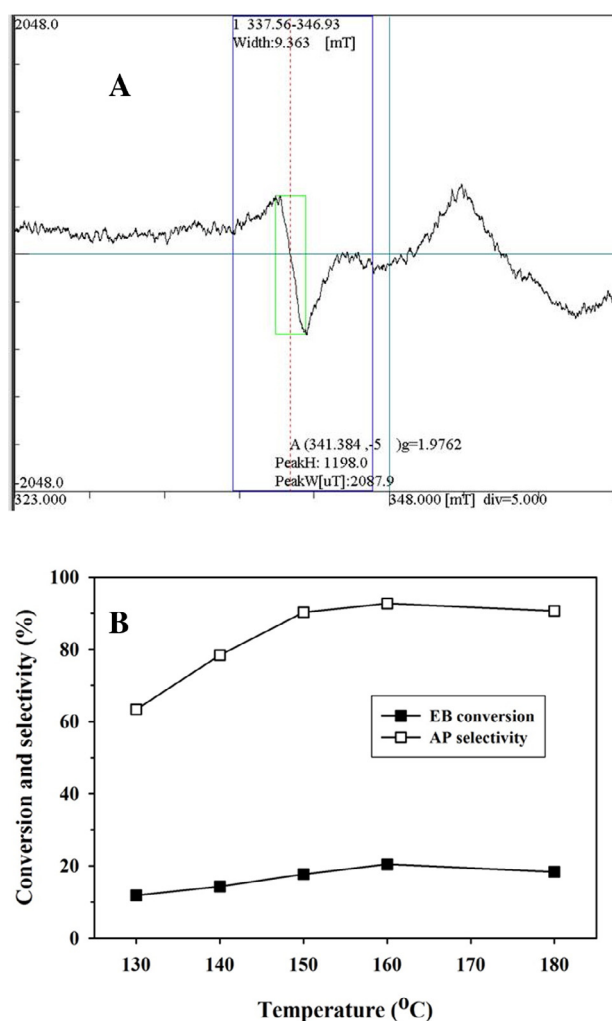
Figure 4 (A) ESR spectrum of Ce-BTC, (B) EB conversion and AP selectivity over Ce-BTC at various temperatures.
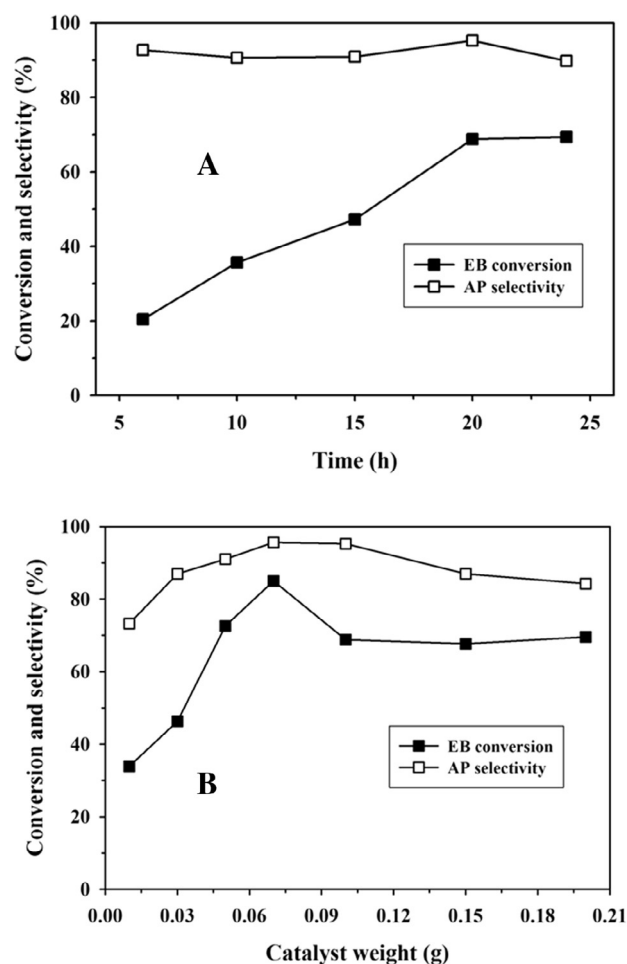

Figure 5 (A) EB conversion and AP selectivity over Ce-BTC at various reaction times, (B) EB conversion and AP selectivity over Ce-BTC at various catalyst weights.

during the process. Bands for —OCO— asymmetric and symmetric stretching were observed at 1644 and 1373 cm^{-1}. $C=C$ stretching of the aromatic rings appeared at 1587 and 1450 cm^{-1}. Additionally, low intensity bands of Ce-O stretching vibrations were seen near 400 and 700 cm^{-1} (Preetha and Janardanan, 2012).

DRS-UV spectra of the catalyst are shown in Fig. 3(B). The peak at 250 nm is due to the $Ce^{3+} \leftarrow O^{2-}$ transition, which is needed for oxidation. The absence of a band at 297 nm demonstrates that there is no $Ce^{4+} \leftarrow O^{2-}$ charge transfer complex formed in the framework, as was found in an earlier report (Rao and Sahu, 2001). The broad envelope peak at 1.97 g in

ESR spectra (Fig. 4(A)) of Ce-BTC also gives an evidence of the presence of a Ce^{3+} phase with an oxygen-adsorbed condition, matching that in a previous study on Ce-doped metal composites and other catalysts (Subbiah et al., 2011).

3.2. Catalytic activity studies

The oxidation of EB was carried out at 160 °C using Ce-BTC as catalyst under solvent-free condition. As one of the reactant is liquid i.e. EB which was acted here as the medium of reaction. For comparison, the reaction was also carried out in the absence of a catalyst. The major expected product of EB

Table 1 EB oxidation reaction catalyzed by Ce-BTC.

| Catalyst	Ethylbenzene conversion (%)	Product selectivity (%)		
		AP	BZ	BA
/	5.01	57.47	6.69	35.84
Ce-BTC	17.67	90.26	4.81	4.93

Temperature: 160 °C, reaction time: 6 h, catalyst weight: 0.10 g, O_2 flow rate: 5.5 ml/min.

oxidation was acetophenone (AP), with a small amount of benzaldehyde (BZ) and benzoic acid (BA), as shown in Table 1. Only 5.01% conversion was achieved without a catalyst, while in the presence of the catalyst both EB conversion and AP selectivity increased. In particular, AP selectivity reached 90.26%. Fig. 4(B) confirms the effect of temperature on the reactions; it shows that the conversion of EB and selectivity of AP increased from 130 to 160 °C, and then a slight decrease was observed at a temperature of 180 °C. Thus, to obtain a higher conversion and selectivity toward AP, 160 °C was chosen as an appropriate reaction temperature for the oxidation of EB over Ce–BTC.

From Fig. 5(A), it is evident that EB conversion increased by increasing the time of the reaction from 6 to 20 h and then reaching a steady state. The maximum conversion of 68.75% was achieved at 20 h. The selectivity of AP also increased with an increase in reaction time. However, the difference was not as large as that found with respect to conversion. As is indicated in Fig. 5(A), over 90% selectivity was achieved at all selected reaction times, and it reached a maximum value of 95.27% at 20 h. The results showed that even at a short reaction time, high product selectivity (>90%) was achieved, while the conversion was more dependent on reaction time. However, from an industrial point of view, conversion and selectivity are equally important. Thus, 20 h was chosen as the optimum reaction time. The conversion and selectivity achieved were less than those reported using Ce-AlPO-5 (Subbiah et al., 2011). The lower conversion is likely due to the reaction here, which was in an atmosphere of oxygen over the liquid phase. The conversion may increase if the reaction was carried out by bubbling the oxygen into the liquid; Ce^{3+} sites on the catalyst may act more efficiently in the conversion. Similarly, the decrease in the

selectivity compared to that found in earlier reports may be due to the retention of the intermediate 1-phenylethanol over the catalyst for a longer period of time. This restricts the diffusion of a new entrant (ethylbenzene) into the pores, leading to exhaustive oxidation of the intermediate into benzaldehyde and benzoic acid. These intermediates were not observed in earlier reports.

As shown in Fig. 5(B), both the conversion of EB and the selectivity of AP increased with an increase in the catalyst quantity, from 0.01 to 0.07 g, and thereafter it decreased. The low conversion and selectivity at lower catalyst weight were caused by insufficient catalyst active sites, while the conversion and selectivity decreased when the catalyst weight was more than 0.07 g and were likely due to the abundant amount of nascent oxygen released from the active sites, which ultimately proceeded to vigorously oxidize and produce products other than AP. When 0.07 g of catalyst was loaded, the conversion and selectivity were 84.99% and 95.63%, respectively. As reported earlier, a plausible mechanism for the reaction is given in Scheme 1 (Subbiah et al., 2011). With respect to the mechanism, in the first step, the Ce^{3+} site will adsorb the O_2 and then form a metal hydroperoxide by abstracting the proton of the $-CH_2-$ group of ethylbenzene where, compared with the methyl proton, the methylene proton is more susceptible to oxidation due to the overcrowding of CH_3 versus $-CH_2-$. Further, the methyl group rotates more than $-CH_2-$, and this restricted rotation by benzene makes it more susceptible to oxidation, as reported earlier. In the next step, the 1-phenylethanol formed will be attacked by atomic oxygen produced by the Ce^{3+} site, causing the expelling of hydrogen in the form of water and producing AP. If the intermediate 1-phenylethanol resides over the catalyst for a long time, it may cause extensive oxidation to other products, such as benz-
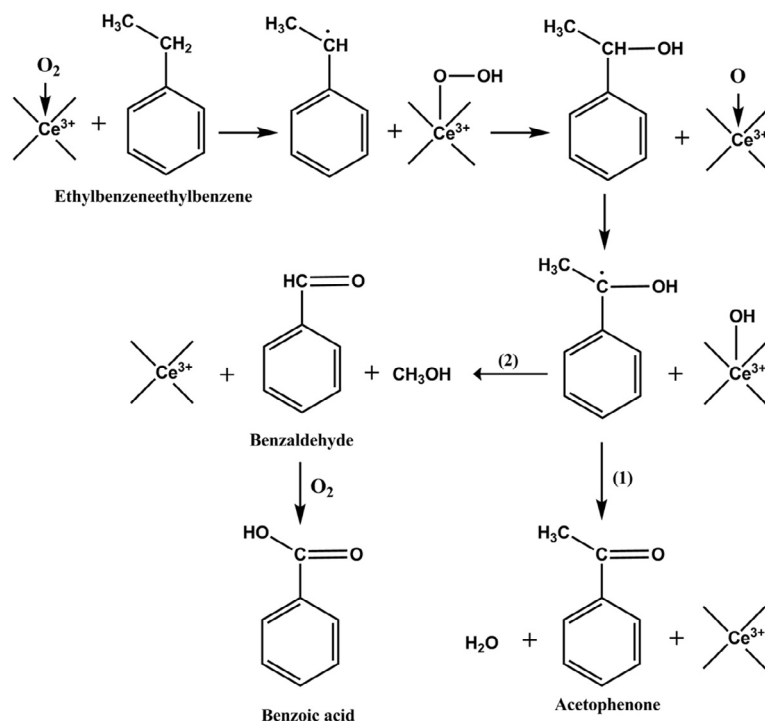
Scheme 1 Possible reaction mechanism for the oxidation of EB over Ce-BTC.

Table 2 Recyclability of Ce–BTC.

Catalyst	Run	EB conversion (%)	Product selectivity (%)		
			AP	BZ	BA
Ce-BTC	1	84.99	95.63	3.87	0.50
	2	82.54	95.60	3.88	0.52
	3	80.34	95.96	3.50	0.54
	4	79.72	95.84	3.67	0.49

Temperature: 160 °C, reaction time: 20 h, catalyst weight: 0.07 g, O_2 flow rate: 5.5 ml/min.

aldehyde and benzoic acid. An earlier report showed a high selectivity for AP due to the use of air as the oxidant where the O_2 quantity is much lower; thus, a slower reaction will proceed to give the desired product with higher conversion (Subbiah et al., 2011). In the present work, we studied the oxidation using pure oxygen. There is more reactive O_2 available here, and the quantity of intermediate formed will rapidly be converted into other products, leading to a small decrease in selectivity.

The next notable property related to using a heterogeneous catalyst is the reusability of that catalyst. Thus, in the present study the catalyst recovered from the first cycle was subjected to two subsequent runs. The results obtained (Table 2) demonstrated that the catalyst activity remained unchanged, but the pore volume was slightly reduced ($0.1062 \ m^3 \ g^{-1}$) from the initial catalyst. This may be due to the presence of small amounts of reactant or product AP (the boiling point of which is 202 °C, which is higher than the catalyst activation temperature) formed during the reaction, indicating that active Ce^{3+} sites responsible for oxidation are present on the surface and not inside the pores as expected. This can be further confirmed from the decrease in peak intensity in DRS-UV spectra (Fig. 3(B)) of Ce-BTC. The decrease in intensity may be due to the presence of AP near the Ce^{3+} site which mask/interfere with the intensity of light absorbance by the Ce^{3+} site. With respect to this mechanism, further investigation is now underway in lab.

4. Conclusions

A cerium based 1,3,5-benzenetricarboxylic acid ligand metal–organic framework Ce-BTC was synthesized and tested as a catalyst for the aerobic oxidation of EB. The results showed evidence that the catalyst was more efficient in the oxidation of the alkyl aromatics tested, with 84.99% conversion and 95.63% selectivity for AP. Moreover, the catalyst was more stable and could be reused for more than four cycles. In addition, Ce-BTC can be used for the oxidation of other alkyl aromatics such as toluene, dimethylbenzene, and diphenylmethane, which are targeted in our future work.

Acknowledgements

Appendix A. Supplementary data

Supplementary data associated with this article can be found, in the online version, at http://dx.doi.org/10.1016/j.arabjc. 2014.11.024.

References

Almáši, M., Zeleňák, V., Císařová, I., Bell, A., 2010. A novel cerium metal-organic framework. http://photon-science.desy.de/annual_-report/files/2010/20101138.pdf.

Araujo, A.S., Aquino, J.M.F.B., Souza, M.J.B., Silva, A.O.S., 2003. Synthesis, characterization and catalytic application of cerium-modified MCM-41. J. Solid State Chem. 171 (1–2), 371–374.

Baver, K., Garbe, D., 1985. Common Fragrance and Flavor Material. VCH Publishers, Weinheim.

Bennur, T.H., Srinivas, D., Sivasanker, S., 2004. Oxidation of ethylbenzene over "neat" and zeolite-Y-encapsulated copper tri- and tetra aza macrocyclic complexes. J. Mol. Catal. A: Chem. 207 (2), 163–171.

David, F., Sonia, A., Catherine, P., 2009. Metal-organic frameworks: opportunities for catalysis. Angew. Chem. Int. Ed. 48 (41), 7502–7513.

Emmanuel, H., Sankar, N., David, S.S., 2010. Efficient calculation of diffusion limitations in metal organic framework materials: a tool for identifying materials for kinetic separations. J. Am. Chem. Soc. 132 (21), 7528–7539.

Françesc, X.L.i.X., Alberto, A., Avelino, C., Hermenegildo, G., 2007. MOFs as catalysts: activity, reusability and shape-selectivity of a Pd-containing MOF. J. Catal. 250 (2), 294–298.

Gao, S.X., Zhao, N., Shu, M.H., Che, S.N., 2010. Palladium nanoparticles supported on MOF-5: a highly active catalyst for a ligand- and copper-free Sonogashira coupling reaction. Appl. Catal. A: Gen. 388 (1–2), 196–201.

Habibi, D., Faraji, A.R., Arshadi, M., Heydari, S., Gil, A., 2013. Efficient catalytic systems based on cobalt for oxidation of ethylbenzene, cyclohexene and oximes in the presence of N-hydroxyphthalimide. Appl. Catal. A: Gen. 466, 282–292.

Hadi, H., Hamid, A., Ali, D., Akbar, B., Ali, R.F., Mostafa, M.A., 2013. Au-SH-SiO$_2$ nanoparticles supported on metal-organic framework (Au-SH-SiO$_2$@Cu-MOF) as a sensor for electrocatalytic oxidation and determination of hydrazine. Electrochim. Acta 88, 301–309.

Isaeva, V.I., Tkachenko, O.P., Afonina, E.V., Kozlova, L.M., Kapustin, G.I., Grünert, W., Solov'eva, S.E., Antipin, I.S., Kustov, L.M., 2013. 2-Butyne-1,4-diol hydrogenation over palladium supported on Zn^{2+}-based – MOF and host–guest MOF/calix[4]arene materials. Micropor. Mesopor. Mater. 166, 167–175.

Jihyun, A., Steven, J.G., Nathaniel, L.R., 2009. Cation-triggered drug release from a porous zinc–adeninate metal–organic framework. J. Am. Chem. Soc. 131 (24), 8376–8377.

Kanjina, W., Trakarnpruk, W., 2010. Oxidation of cyclohexane and ethylbenzene by hydrogen peroxide over Co-substituted hetero-polytungstate catalyst. J. Met. Mater. Miner. 20, 29–34.

Keigo, K., Jun, K., Kazuya, Y., Noritaka, M., 2004. Efficient heterogeneous oxidation of alkylarenes with molecular oxygen. Org. Lett. 6 (20), 3577–3580.

Kroschwitz, J.I., Howe-Grant, M. (Eds.), 1995, 4th Ed. K.O. Encyclopedia of Chem. Techn., New York.

Lida, H., Faezeh, F., 2013. Cobalt metal organic framework as an efficient heterogeneous catalyst for the oxidation of alkanes and alkenes. React. Kinet. Mech. Catal. 109 (1), 67–75.

Lien, T.L.N., Chi, V.N., Giao, H.D., Ky, K.A.L., Nam, T.S.P., 2011. Towards applications of metal–organic frameworks in catalysis: Friedel-Crafts acylation reaction over IRMOF-8 as an efficient heterogeneous catalyst. J. Mol. Catal. A: Chem. 349 (1–2), 28–35.

Lien, T.L.N., Tung, T.N., Khoa, D.N., Nam, T.S.P., 2012. Metal–organic framework MOF-199 as an efficient heterogeneous catalyst for the aza-Michael reaction. Appl. Catal. A: Gen. 425–426, 44–52.

Lu, C.L., Fu, Z.H., Liu, Y.C., Liu, F.L., Wu, Y.Y., Qin, J.W., He, X.L., Yin, D.L., 2010. A moderate and efficient method for oxidation of ethylbenzene with hydrogen peroxide catalyzed by 8-quinolinolato manganese (III) complexes. J. Mol. Catal. A: Chem. 331 (1–2), 106–111.

Luo, J.H., Xu, H.G., Liu, Y., Zhao, Y.S., Daemen, L.L., Brown, C., Timofeeva, T.V., Ma, S.Q., Zhou, H.C., 2008. Hydrogen adsorption in a highly stable porous rare-earth metal-organic framework: sorption properties and neutron diffraction studies. J. Am. Chem. Soc. 130 (30), 9626–9627.

Luz, I., León, A., Boronat, M., Llabrés i Xamena, F.X., Corma, A., 2013. Selective aerobic oxidation of activated alkanes with MOFs and their use for epoxidation of olefins with oxygen in a tandem reaction. Catal. Sci. Technol. 3, 371–379.

Ma, S.Q., Zhou, H.C., 2010. Gas storage in porous metal–organic frameworks for clean energy applications. Chem. Commun. 46, 44–53.

Matthias, V., Shyam, B., Karen, L., Joachim, P., Joachim, S., Toon, V., Pascal, V.D.V., Michel, W., Veronique, V.S., 2014. Catalytic performance of vanadium MIL-47 and linker-substituted variants in the oxidation of cyclohexene: a combined theoretical and experimental approach. ChemPlusChem 79 (8), 1183–1197.

Mikaela, G., Agnieszka, B., Belén, M.M., Sun, J.L., Jekabs, G., Tony, Z., Li, Z.Y., Zhu, G.S., Zou, X.D., 2010. A family of highly stable lanthanide metal–organic frameworks: structural evolution and catalytic activity. Chem. Mater. 22 (11), 3316–3322.

Nazmul, A.K., Md, M.H., Sung, H.J., 2010. Accelerated syntheses of porous isostructural lanthanide-benzenetricarboxylates (Ln–BTC) under ultrasound at room temperature. Eur. J. Inorg. Chem. 2010 (31), 4975–4981.

Nicholson, J.S., Adams, S.S., 1968. Phenyl propionic acids. U.S. Patent 3, 385, 886.

Preetha, B., Janardanan, C., 2012. UV–visible diffuse reflectance spectroscopic studies on Mn and Cu ion exchange of newly synthesized cerium zirconium antimonate and its application in dye degradation. Res. J. Recent Sci. 1, 85–92 (ISC-2011).

Raju, G., Reddy, P.S., Ashok, J., Reddy, B.M., Venugopal, A., 2008. Solvent-free aerobic oxidation of ethylbenzene over supported Ni catalysts using molecular oxygen at atmospheric pressure. J. Natural Gas Chem. 17 (3), 293–397.

Rao, G.R., Sahu, H.R., 2001. XRD and UV–Vis diffuse reflectance analysis of CeO_2–ZrO_2 solid solutions synthesized by combustion method. J. Chem. Sci. (Indian Acad. Sci.) 113 (10-12), 651–658.

Shrikant, S.B., Shylesh, S., Kamble, K.R., Singh, A.P., 2006. Cobalt-containing hexagonal mesoporous molecular sieves (Co-HMS): synthesis, characterization and catalytic activity in the oxidation reaction of ethylbenzene. J. Mol. Catal. A: Chem. 255 (1–2), 123–130.

Song, F.J., Wang, C., Joseph, M.F., Ma, L.Q., Lin, W.B., 2010. Isoreticular chiral metal−organic frameworks for asymmetric alkene epoxidation: tuning catalytic activity by controlling framework catenation and varying open channel sizes. J. Am. Chem. Soc. 132 (43), 15390–15398.

Subbiah, D., Muthiahpillai, P., Velayutham, M., 2011. Selective oxidation of ethylbenzene over CeAlPO-5. Appl. Catal., A 407 (1-2), 76–84.

Vasant, R.C., Jayant, R.I., Vijay, S.N., Rani, J., 2004. MnO_4^{-1} exchanged Mg–Al hydrotalcite: a stable and reusable/environmental-friendly catalyst for selective oxidation by oxygen of ethylbenzene to acetophenone and diphenylmethane to benzophenone. J. Catal. 227 (1), 257–261.

Zhang, C.Y., Wang, M.Y., Liu, L., Yang, X.J., Xu, X.Y., 2013. Electrochemical investigation of a new Cu-MOF and its electro-catalytic activity towards H_2O_2 oxidation in alkaline solution. Electrochem. Commun. 33, 131–134.

Zhao, R., Wang, Y.Q., Guo, Y.L., Guo, Y., Liu, X.H., Zhang, Z.G., Wang, Y.S., Zhan, W.C., Lu, G.Z., 2006. A novel Ce/AlPO-5 catalyst for solvent-free liquid phase oxidation of cyclohexane by oxygen. Green Chem. 8, 459–466.

Zhou, Y.X., Song, J.L., Liang, S.G., Hu, S.Q., Liu, H.Z., Jiang, T., Han, B.X., 2009. Metal-organic frameworks as an acid catalyst for the synthesis of ethyl methyl carbonate via transesterification. J. Mol. Catal. A: Chem. 308 (1–2), 68–75.